Damage in high cycle fatigue
- From isotropic accumulation to spatial discrete distribution of damage -

Laurent Flacelière[a], Franck Morel[b],and André Dragon[c]

[a] ASCOMETAL-CREAS, BP 70045, 57301 Hagondange Cedex, France
l.flaceliere@ascometal.lucchini.com
[b] ENSAM., Laboratoire Procédés Matériaux Instrumentation (LMPI), EA 1427,
2 boulevard du Ronceray, BP 93525, 49025 Angers Cedex, France.
[c] ENSMA., Laboratoire de Mécanique et de Physique des Matériaux (LMPM), UMR 6617,
BP 109, 86960 Futuroscope Cedex, France.

Abstract The effect of cyclic loading on metallic components concerns a high number of industrial applications but is difficult to analyse because of the data scatter observed in service. Moreover, this damage mode is very sensitive to the stress state, the mean level and the loading path. The loading history subjected to a structure is then essential to estimate the life potential available for the user.

The physical characterization of the mesocrack activity is the first goal of this work, not exposed here. Some SEM observations are hence carried out both for simple and complex loadings. The damage interaction mechanisms between cracks is more especially investigated, these cracks being initiated or propagated by the application of different loading conditions. The fields of the limited and unlimited endurance are explored (lifetimes between 10^5 and 10^6 cycles). The predictions of the suggested modelling are compared to the observations of the initiation and growth of the damage related to various stress paths.

The second goal is the development of a model built in the framework of damage mechanics and able to describe the grain degradation due to the initiation crack phase. This approach uses a strong coupling between damage and the cyclic plastic behaviour of the crystal at the mesoscopic scale. These models are inspired by well-known approaches trying to get the local cyclic behaviour of grains in polycrystalline aggregates (Dang Van, Papadopoulos, Morel). A thermodynamic framework is used to guide construction of theses models.

Whatever the loading mode applied, it is possible to get the residual lifetime by knowing the damage value reached. The extension of the lifetime can be imagined by perfectly handling the damage interaction laws between loading modes, and a coupling with a probabilistic approach can allow to estimate the strength potential with respect to the damage.

1 INTRODUCTION

Many attempts have been made to describe the damage evolution of damage for metallic materials submitted to high cycle fatigue (HCF), as well as for uniaxial or multiaxial loading conditions. In HCF, damage can be considered as a process of progressive deterioration of the material, at the mesoscopic scale [1]. Of course, applied stress, microstructure or elaboration process have strong influences on the damage development.

Consequently, several modelling were interested in the description of damage initiation and development in the HCF regime, following varied complexity levels. For example, it is possible to use only one scalar quantity as well as superior order damage tensors (order 2 or 4) to represent the damage [2]. Moreover, the consideration of one or several scales (based on localization processes due to micromechanics framework), induce more or less complex proposals. Well-known proposals are the phenomelogical model of Chaboche (isotropic damage, use of effective stress) [3], the two scales Lemaitre model (isotropic damage based on localization at mesoscopic scale) [4], the model of Mroz (anisotropic damage description at macroscopic scale) [5], or the work of Abdul_Latif (three scales, damage representation based on the grain slip directions) [6].

The main goal of this work is to develop a new approach proposing a reasonable compromise between efficient damage representation and simplicity. After a first proposal based on isotropic damage distribution, two enriched proposals in terms of damage description will be introduced to account for HCF damage observed. An other purpose of this study is to measure how an advanced description can account for the complex effects of cumulative damage effects under multiaxial loading. This is done by keeping in mind the increase of the complexity for the parameters identification and the numerical implementation.

2 MESOSCOPIC PLASTIC-DAMAGE COUPLED APPROACH

A clear distinction between the plasticity and damage effects on the physically representative scales is assumed, and this distinction is made intuitively according to the major cause of degradation of material properties [1]. The two related phenomena are coupled and this feature must be carefully examined.

The damage mechanics considers the concept of 'delocalized' defects, that is defects whose physical presence has not necessarily been confirmed [2]. This leads to the study of early effects with respect to what happens at the end of the life of the sample, even before a dominant macrocrack occurs. As stated by McDowell [7], during the initiation phase, damage can be considered as homogeneous in the representative elementary volume (RVE). This fact authorizes the use of the "Continuum Damage Mechanics" (CDM).

The use of a scale lower than the macroscopic scale is justified by the nature of the physical mechanisms. This compromise, embodied by a localisation rule, allows to determine the mesoscopic stress and strain from their macroscopic counterparts the latter being accessible by the engineer. For the sake of simplicity [8], the Lin-Taylor proposal (1) is used :

$$\underline{\underline{\sigma}} = \underline{\underline{\Sigma}} - 2\mu \underline{\underline{\varepsilon}}^{p} \tag{1}$$

where $\underline{\underline{\sigma}}$ and $\underline{\underline{\varepsilon}}^{p}$ represent the stress and plastic strain tensors at the mesoscopic scale and $\underline{\underline{\Sigma}}$ is the macroscopic stress tensor.

The framework of irreversible thermodynamics with internal variables for time-independent, isothermal transformations and small deformations is used. The model is built by assuming the existence of a thermodynamic potential, namely free energy, as well as the existence of dissipation potentials involving distinct multipliers, a normal dissipation being postulated for each mechanism (plasticity, damage) while the evolution laws regarding plasticity are governed by associated rules (not so for damage). The choice of a priori uncoupled dissipations for plasticity and damage makes it easier to distinguish between the mechanisms concerned and the two criteria. This choice leads to local plastic straining before any damage development.

2.1 Purely isotropic description (model A)

The elastic and inelastic parts of the granular specific free energy can be written as (2) and (3).

$$\omega = \rho\psi = \omega^{e}\left(\underline{\underline{\varepsilon}}^{e}\right) + \omega^{p}\left(\underline{\underline{\varepsilon}}^{p}, p, d\right) + \omega^{d}(d, \beta) \tag{2}$$

$$\omega = \frac{1}{2}\left(\underline{\underline{\varepsilon}} - \underline{\underline{\varepsilon}}^{p}\right) : \underline{\underline{\underline{\underline{C}}}} : \left(\underline{\underline{\varepsilon}} - \underline{\underline{\varepsilon}}^{p}\right) + \frac{1}{2} c \underline{\underline{\alpha}} : \underline{\underline{\alpha}} + \tilde{r}_{\infty} p \exp(-sd) + \frac{\tilde{r}_{\infty}}{g} \exp(-gp)\exp(-sd) + F_{d0} d + \frac{1}{2} q \beta^{2} \tag{3}$$

The intrinsic dissipation, at the grain level is given below by equation (4).

$$\Phi = \underline{\underline{\sigma}} : \dot{\underline{\underline{\varepsilon}}}^{p} - \underline{\underline{x}} : \dot{\underline{\underline{\alpha}}} - r.\dot{p} + F_{d}\dot{d} - k\dot{\beta} \geq 0 \tag{4}$$

The conjugate forces relative to kinematic and isotropic local hardening mechanisms are more classic.

$$\underline{\underline{x}} = \frac{\partial \omega}{\partial \underline{\underline{\alpha}}} = c\underline{\underline{\alpha}} = c\underline{\underline{\varepsilon}}^{p} \tag{5}$$

$$r = \frac{\partial \omega}{\partial p} = r_{\infty}\left(1 - \exp(-gp)\right)\exp(-sd) \tag{6}$$

In the last expression, r_{∞} designates the saturation isotropic value of the force r, g is the hardening parameter and s is a damage sensitivity parameter. This relation incorporates specific coupling effects between plasticity and damage at a local scale. As the damage increases, the isotropic hardening becomes weaker, but the kinematic hardening is not affected by damage, and remains active. The isotropic part of the hardening then tends to vanish and a local elastic shakedown state is impossible to reach, leading to the failure. F_d is the conjugate force corresponding to the damage variable d. This force depends both on the accumulated plastic strain p and the damage d, and is derived from equation (7).

$$F_{d} = -\frac{\partial \omega}{\partial d} = \tilde{r}_{\infty} s \exp(-sd)\left(p + \frac{\exp(-gp)}{g}\right) \tag{7}$$

$$k = -\frac{\partial \omega}{\partial \beta} = q\beta \tag{8}$$

A second scalar variable, denoted as β, is defined as the measure of 'cumulated damage'. Its conjugate force is denoted as k and depends linearly on β (8). The plastic yield condition at the mesoscopic scale is given by (9), where $\underline{\underline{s}}$ is the mesoscopic stress deviator.

$$f\left(\underline{\underline{\sigma}}, \underline{\underline{x}}, r\right) = J_2{}'\left(\underline{\underline{s}} - \underline{\underline{x}}\right) - \left(r + r_0\right) = 0 \qquad (9)$$

A nonassociated law is assumed concerning damage evolution; the damage loading function is hence distinct from the damage potential H. Equation (10) gives the damage loading function h, where a is the hydrostatic stress sensitivity coefficient for the damage threshold, and k_0 is the initial damage threshold, while k governs the damage threshold evolution. The function H (11) shows a similar expressions but exhibits a different hydrostatic stress sensitivity parameter b governing the damage developpement.

$$h\left(F_d, k; \sigma_h\right) = F_d\left(1 + a\sigma_h\right) - \left(k + k_0\right) \leq 0 \qquad (10) \qquad\qquad H\left(F_d, k; \sigma_h\right) = F_d\left(1 + b\sigma_h\right) - \left(k + k_1\right) \qquad (11)$$

This model shows two distinct scalar variables regarding damage : d describes more specifically the damage effect on material properties (isotropic hardening), by controlling the elastic surface radius. The second variable, β, is a cumulated damage measure, and corresponds to the creation of new decohesion surfaces (mesocracking). This use of two variables to describe the complexity of the damage is close to the proposal of Cordebois and Sidoroff [9]. The damage variable β and the damage effect variable d evolve in convergent or divergent manner depending on the stress-path (12).

$$\beta = \frac{\dot{d}}{\left(1 + b\sigma_H\right)} \qquad (12)$$

2.2 Modelling included crack bifurcation (model B)

The principal improvement of this second modelling is to take into account the crack orientation changing (branches), from the maximal shear stress (mode II) to the normal or the maximal principal stress (mode I).

Without detailing each equation, it can be said that this model B uses an elastoplastic description identical to model A for the localization phases. But, two damage mechanisms are modelled, each having its own activation threshold and evolution. These damage descriptions remain isotropic, but make it possible to distinguish cracks in mode I from cracks in mode II. For uniaxial loading without complex cumulative effect, these mode I and mode II of damage can easily be associated to observed crack orientations.

This model B uses, for sake of simplicity, associated damage description. The mesoscopic free energy (Gibbs) for the model B is given by the expression (13).

$$\omega^* = \frac{1}{2}\left[\frac{1+\nu}{E}\underline{\underline{s}} : \underline{\underline{s}} + 3\frac{1-2\nu}{E}\sigma_H^2 \exp(ed_I)\right] - \frac{1}{2}c\underline{\underline{\alpha}} : \underline{\underline{\alpha}} - \tilde{r}_\infty p \exp(-s_I d_I)\exp(-s_{II} d_{II}) - \frac{\tilde{r}_\infty}{g}\exp(-gp)\exp(-s_I d_I)\exp(-s_{II} d_{II}) - r_0\, p - \frac{1}{2}q_{II}\beta_{II}^2 \qquad (13)$$

The mode II damage, activated before the mode I damage, independent and non simultaneous of the mesoplastic flow, is close to the model A, and integrates at the same time the effects of d_I and d_{II}.

$$r = -\frac{\partial\omega^*}{\partial p} = \tilde{r}_\infty\left(1 - \exp(-gp)\right)\exp\left(-s_I d_I\right)\exp\left(-s_{II} d_{II}\right) + r_0 \qquad (14)$$

The mode II damage modelling is given by the equations (15), (16) and (17), whereas the equation (18) and (19) describe the mode I damage modelling.

Mode II	Mode I
$h\left(F_d, k; \sigma_h\right) = F_{d_{II}}\left(1 + a\sigma_h\right) - \left(k + k_0\right)$ (15)	$g\left(F_{d_I}; d_I\right) = F_{d_I} - \left(q_I d_I + k_{01}(\sigma_{H,\max})\right)$ (18)
$F_{d_{II}} = \tilde{r}_\infty s_{II} \exp\left(-s_I d_I\right)\exp\left(-s_{II} d_{II}\right)\left(p + \frac{\exp(-gp)}{g}\right)$ (16)	$F_{d_I} = \frac{3(1-2\nu)}{2E}\sigma_h^2 e\exp(ed_I) + r_\infty s_I \exp\left(-s_I d_I\right)\exp\left(-s_{II} d_{II}\right)\left(p + \frac{\exp(-gp)}{g}\right)$ (19)
$k_{II} = \frac{\partial\omega^*}{\partial\beta_{II}} = q_{II}\beta_{II}$ (17)	

It is to be noticed that this transition from the mode II damage description to the mode I damage description is a way to modulate the hydrostatic stress effects during the initiation and the propagation phase of cracks. Thus, mode II is directly influenced by the value of σ_H, whereas mode I is controlled by its maximum value during the cycle, noted $\sigma_{H,max}$, close to the linear failure mechanics concept, suitable for the propagation in mode I.

2.3 Spatial discrete damage distribution modelling (model C)

The goal of this third proposal is to take into account the spatial damage distribution. The branching phenomenon of cracks is always considered, and takes a reinforced physical significance. Moreover, the cumulative damage effect, following various space directions, is different from that carried out by the two last models.

This model is based on a "multiple" approach. Consequently, all mechanical used quantities (variables, forces and parameters) are specific for each considered plane. Thus, this model generates as many damage values as the considered systems ($\underline{n}$, $\underline{m}$).

One main evolution proposed by the model C is to take into account, at the mesoscopic scale, the plastic slip direction where the mode II damage progresses. This description is based on a Schmid criterion, often used in HCF. Some experimental results showed a good correlation with this criterion, with a notable prediction improvement, for few materials, compared to the volumic Von Mises approach. For mode II, the resolved shear stress in the considered slip system is first calculated, by using the orientation vector of slip direction $\underline{m}$ (20). The localization relation of Lin-Taylor, projected on the system ($\underline{n}$, $\underline{m}$), is given by (21).

$$\underline{\tau} = \left(\underline{\underline{\sigma}} : \underline{\underline{a}}\right)\underline{m} \qquad (20) \qquad\qquad \underline{\tau} = \underline{T} - \mu \underline{\gamma}^p \qquad (21)$$

In the same way, quantities used for mode II in the model C are colinear vectors to the direction $\underline{m}$. Thus plastic strain is quantified by the plastic slip vector $\underline{\gamma}^p$, and the localization scheme uses the macroscopic resolved shear stress $\underline{T}$. Note that the macroscopic stress normal to the crack ("opening stress"), noted $\underline{\Sigma}_n$, is integrally transmitted to the mesoscopic scale. Moreover, for mode II, this modelling induces a total independence between plastic slip directions. Practically, the activation of a new plastic slip direction is done without considering other already activated directions. Physically, this consists in considering a total independence between different orientation accumulation plastic slip systems. Equation (22) gives the energy for this proposal, in terms of stress.

$$\omega^* = \frac{1}{2}\left[\frac{\underline{\sigma}_n . \underline{\sigma}_n}{E}\exp(ed_I^m)\right] - \frac{1}{2}c\underline{\gamma}^p . \underline{\gamma}^p - \tilde{\tau}_\infty p \exp(-s_I d_I)\exp(-s_{II} d_{II}) - \frac{\tilde{\tau}_\infty}{g}\exp(-gp)\exp(-s_I d_I)\exp(-s_{II} d_{II}) - r_0\, p + \frac{1}{2} q_{II} \beta_{II}^2 \qquad (22)$$

Equations (23) to (26) defines elastoplastic crystal behaviour, always in projection on the system ($\underline{n}$, $\underline{m}$), and equation (27) to (29) gives mode II damage threshold and driving force.

$f\left(\underline{\tau}, \underline{b}, r\right) = \sqrt{\left(\underline{\tau} - \underline{b}\right).\left(\underline{\tau} - \underline{b}\right)} - \left(\tau + \tau_0\right) \leq 0$ (23)	$h\left(F_d, k; \sigma_{\underline{n}}\right) = F_{d_{II}}\left(1 + a\sigma_{\underline{n}}\right) - \left(k_{II} + k_0\right)$ (27)
$\underline{e}^{en} = \frac{\partial w^*}{\partial \underline{\sigma}_n} = \frac{\underline{\sigma}_n}{E}\exp(ed_I)$ (24)	$F_{dII} = \frac{\partial \omega^*}{\partial d_{II}} = \tau_\infty s_{II} \exp\left(-s_I d_I\right)\exp\left(-s_{II} d_{II}\right)\left(p + \frac{\exp(-gp)}{g}\right)$ (28)
$\underline{b} = -\frac{\partial \omega^*}{\partial \underline{\gamma}^p} = c\underline{\gamma}^p$ (25)	$k_{II} = \frac{\partial \omega}{\partial \beta_{II}} = q_{II} \beta_{II}$ (29)
$\tau = -\frac{\partial \omega^*}{\partial p} = \tau_\infty\left(1 - \exp(-gp)\right)\exp\left(-s_I d_I\right)\exp\left(-s_{II} d_{II}\right) + r_0$ (26)	

The mode I modelling used what was done for the model B. In particular, a volumic plastic description was retained, associated, for damage, with the opening stress σ_N.

This choice offers the possibility of writing close formalisms for mode II and mode I. The passage of projected quantities according to volumic quantities implies only adaptation of the selected formalism. It is necessary to establish continuity conditions for used variables. Hence, for the suggested model, the variable p, for a given direction, is regarded as continuous from the mode II to the mode I. Damage variables, by construction, are discontinuous from one mode to another.

Moreover, the assumptions that $\tau = r$ ensures, for a pure torsion loading, continuity of the plastic flow during the branches, justifying the interest of J2 measurement homogeneous to a shear stress. For other tested loading, inducing hydrostatic stress, the discontinuities of the plastic flow remained low (influence on less than 10^4 cycles). In addition, as well in mode I or in mode II, all damage effects on elastic or plastic behaviour remain identical to the description done with the model B.

3 COMPARISON OF THE PREDICTIONS OBTAINED BY EACH APPROACH

After the presentation of theses three proposals, it is proposed to use them for lifetime prediction of samples made of a C35 mild steel. The tests carried out allows the possibility of conducting a correct identification of the parameters related to these models. During the identification procedure, only part of the data resulting from the tests will be used, in order to leave available, for the comparison, other experimental results. These results were selected among the most complex tests, such as those with mean stress, block loading. The evolutions and enrichments brought by each of three proposals are the result of confrontations and interactions with the numerical predictions of these models.

For the parameter identification, the procedure begins with parameters related to the model A, which is the simplest of the three suggested models. This identification requires to know the cyclic elastoplastic behaviour curve and two Wöhler curves in purely alternative torsion (R=-1) and purely alternative tension/compression (R=-1). The additional identification of the parameters required by the model B concerns only the mode I, and requires some SEM observations to quantify the lifetime fraction at the crack branching event. The model C, based on slip direction in mode II, uses different stress equivalent measurement. Consequently, this choice generates slightly different identified parameters compared to the first two models.

After this identification process, it is possible to use the other experimental results to confront the models to the data not used during the identification. This confrontation requires tests of higher complexity like combined in phase tension-torsion, or block loading sequences. The first confrontation concerns a test based on a block sequence of tension and torsion, alternated every 10^5 cycles, and beginning by tension (C36I01). The two specimens, loaded at levels involving similar lifetime in simple tension and torsion, give lifetimes respectively of $6{,}27.10^5$ and $6{,}21.10^5$ cycles. The models A, B and C predict respectively lifetimes of $4{,}64.10^5$, $4{,}05.10^5$ and $2{,}62.10^5$ cycles, whereas a standard linear cumulative rule (Miner) predicts a lifetime of $3{,}43.10^5$ cycles.

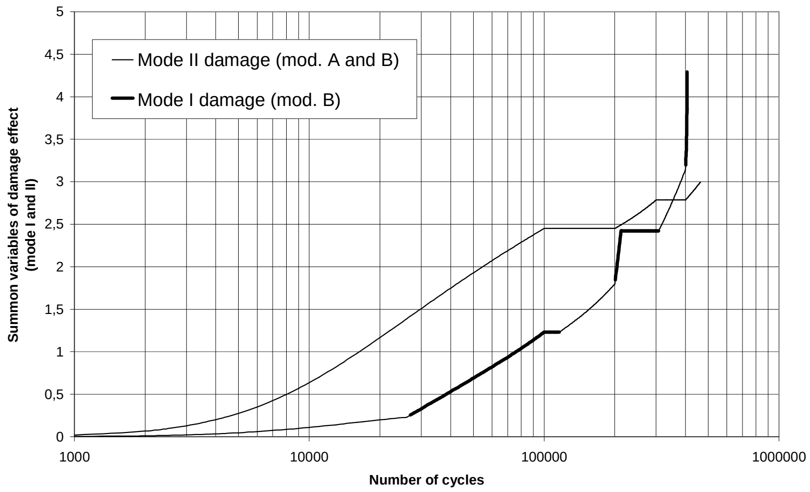

Figure 1. Evolution prediction of the sum of mode I and mode II damage effect variables for the models A and B, in function of the number of cycles, for test C36I01

These results show that, in spite of the activation of several damage directions, the predicted lifetimes by the models B and C are inferior compared to experimental results. The isotropic cumulative effect from the model A induces longer predicted lifetimes. Of course, the very limited number of tested specimens (2 !), does not allow to draw a definitive conclusion from this confrontation. However, in this first case, the enrichment of the damage description does not bring a significant profit in term of quality of the predictions. It just makes it possible to correlate the physical direction of the crack propagation, as it could be seen on Figure 4 and 5.

In order to continue this confrontation, the three models are now confronted to the data from block loading tests. These loading sequences are composed of blocks of pure torsion (To), pure tension (T), or in-phase tension-torsion with two stress ratios ($k=\sigma_{xy,a}/\sigma_{xx,a}$). The stress levels of each loading block were adjusted in order to correspond to a lifetime of 8.10^5 cycles.

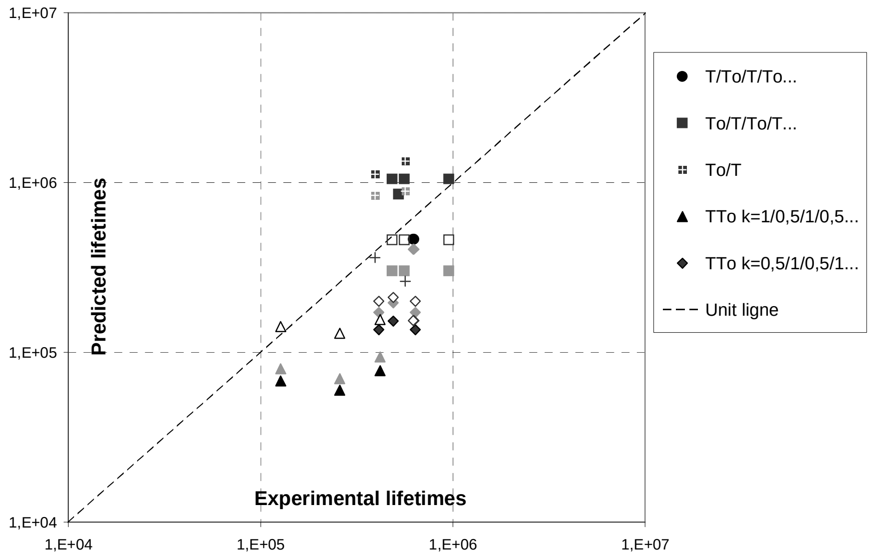

Figure 2. Correlation between experimental and predicted lifetimes for each model, for block loading tests. Black symbols are for model A, grey for model B and white for model C.

Let us focus more particularly to the spatial damage distribution prediction obtained with the model C. Figure 2 illustrates the results provided by the model C for a continuous pure alternating torsion test, according to the two most critical stress planes. This combination of two critical planes is that giving the smallest lifetime for each mode (mode II and mode I). This crack system corresponds to two mode II crack systems, oriented along and perpendicular to the axis of the test specimen, and to two mode I crack systems, at 45° of the specimen axis. Any other direction induces longer lifetime, or lower damage value. That is clear on Figure *3*, giving the predicted damage distribution on the specimen surface in mode I and II, for the same last torsion loading ($\sigma_{zy,\,a}=175Mpa$) and when the failure criterion is reached for the critical direction ($d_I=d_{cI}$ and $d_{II}<d_{cII}$). It appears that the modelling enrichment, while decreasing cumulative damage effect carried out by model A is beneficial. Of course, these results are strongly dependent on the quality of parameters identification related to each model, and of the dispersion specific to HCF tests.

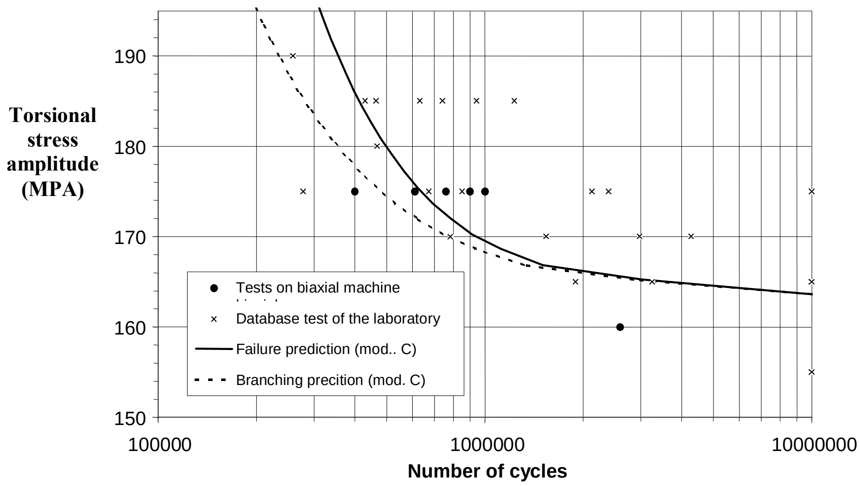

Figure 3. Wöhler curves indicated predicted branching and failure of the crystal by the model C, and experimental points obtained in pure alternate torsion (R=-1)

The correspondence between Figures 4 and 5 shows that the critical mode II and mode I planes are really those on which cracks start and propagate. In addition to the large macroscopic crack on this SEM view, it is possible to distinguish other smaller cracks, started in mode II, and directed along the specimen axis, as envisaged by the predicted damage distribution. The lamella microstructure of this ferrito-perlitic steel induces that the perpendicular direction to the rolling axis of the specimen is most prone to crack propagation.

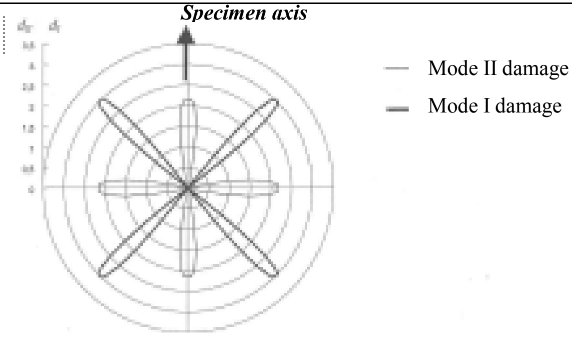

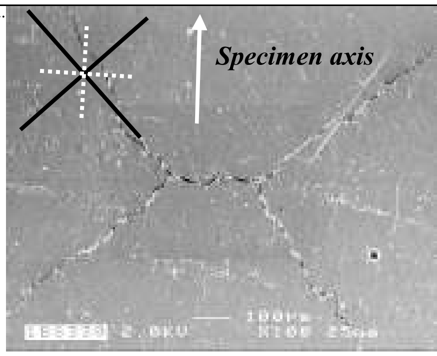

Figure 4 and 5. Spatial damage distribution prediction of the model C, for a pure alternating torsion loading (R=-1, ($\sigma_{zy,\,a}$=175Mpa), and SEM observations for same loading conditions, after 8.10^5 cycles.

Always for blocks loading sequences, the two Figures 6 and 7 of predicted damage distribution illustrate an interesting case of cumulative damage effect. The loading sequence of the specimen C36I06 is based on the sequential application of block of tension-torsion for which stress ratio k varies from one block to another (k=0,5 and k=1), and begins with k=1. In this case, the variations of critical plane directions exist, but are weak, generating a real cumulative damage effect in mode II at the passage from one block to another. This is due to the biggest number of planes experiencing high values of plasticity and damage. In this case, as it could be seen on the Figure 6, the damage distribution is non-symmetrical.

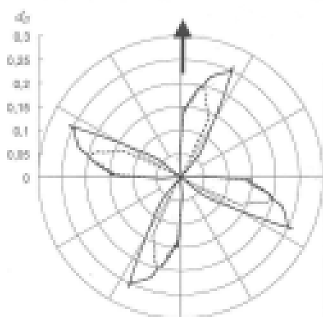

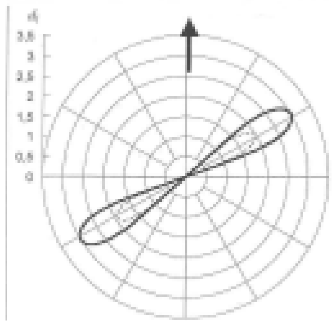

Damage after 105 cycles (end of block k=1)
Predicted damage faillure (after 1,56.105 cycles, during block k=0,5)

Figure 6. Mode II damage variable effect for C36I06 specimen.

Figure 7. Mode I damage variable effect for C36I06 specimen.

4 CONCLUSIONS AND PERSPECTIVES

A framework of irreversible thermodynamics processes with internal variables is employed to build a damage model family, dedicated to multiaxial high cycle fatigue. Local plasticity plays a fundamental role in this fatigue regime; hence some mesoscopic cyclic hardening and damage rules are postulated to reflect this feature. The model leads to the prediction of the fatigue limit (defined as the stress limit under which no initiation occurs) according to the concept of elastic shakedown. It is also able to predict a cyclic behaviour close to plastic shakedown because of a coupling between plasticity and damage. Indeed, when a threshold value of the accumulated plastic strain has been reached, the damage inhibits the yield stress evolution so that only the kinematic part of the hardening remains active. This hardening feature is precisely a condition of plastic shakedown.

Moreover, with this approach, the damage nucleation and growth are governed by non-associated laws for the first isotropic model A. The effect of the hydrostatic stress on the damage threshold is different from its influence on the damage growth. This property is interesting and none of the classical damage rules applied in high cycle fatigue shows this difference. Evolutions of this approach are proposed with the extensions B and C. These last proposals must be regarded as an attempt for an anisotropic damage description.

The damage variables used for the models A and B lead to a total damage accumulation, for each mode of propagation (total damage cumulative effect for mode II, and total damage cumulative effect for mode I in case of the model B). This is the consequence of the use of isotropic variables.

The approach of the model C is of micro-plane type, and considers no damage interaction between the various space directions. That corresponds to a total independence between crack systems, with no cumulative effect between these systems.

Finally, this work shows that the extension to the anisotropic description of an initially purely isotropic model is made easier by the use of "plane" scalar variables. That induces a rather strong independence between each loading directions, in agreement with what can be observed in HCF. The cases of strong interactions between cracks occur for important damages, rather at the end of the lifetime.

SEM observations carried out during this work showed that the crack directions in HCF were defined by the loading mode. This leads to the definition of the critical planes related to mode I and II. By using some foreseeable directions of these critical planes, it is possible to work with a few scalar variables, related to the identified critical directions, and hence simplify the calculations carried out. Moreover, works of Kachanov on the damage description [11] is a way to enrich this type of modelling, especially for mode I.

5 REFERENCES

1. *LEMAITRE, J., A course on damage mechanics, ed. S.V. Ed. 1992.*
2. *DRAGON, A., and HALM, D., Damage mechanics - some modelling challenges -. Amas Lecture notes 9, 2004, Poland.*
3. *CHABOCHE, J.L. and P.M. LESNE, A non-linear continous fatigue damage model. Fatigue Fract. Engng. Mater. Struct., 1988. 11(1): p. 1-17.*
4. *LEMAITRE, J., A continuous damage mechanics model for ductile fracture. Journal of Engineering Materials and Technology, 1985. 107: p. 83-89.*
5. *SEWERYN, A. and MROZ, Z., On the criterion of damage evolution for variable multixial stress states. Solids Structures, 1997. 35(14): p. 1586-1616.*
6. *ABDUL-LATIF, A., and SAANOUNI, K., Damaged anelastic behaviour of FCC polycrystalline metals with micromechanical approach. International Journal of Damage mechanics, 1994. 3:p. 237-259.*
7. *McDOWELL, D.L., Damage mechanics end metal fatigue : a discriminating perspective. International Journal of Damage mechanics, 1999. 8: p. 376-403.*
8. *MOREL, F., A critical plane approach for life prediction of high cycle fatigue under multiaxial variable loading. int. J. Fatigue, 2000(22): p. 101-119.*
9. *CORDEBOIS, J.P. and F. SIDOROFF, Damage induced elastic anisotropy. Colloque Euromech 115, 1979. Villard de Lans, France.*
10. *HAYAKAWA, K. and S. MURAKAMI, Space of damage conjugate force and damage potential of elastic-plastic-damage materials, in Damage mechanics in engineering materials, G.Z. VOYIADJIS, J.-*
11. *KACHANOV, L.M., Time of the rupture process under creep conditions. Isv. Akad. Nauk., Otd Tekh. Nauk., 1958. 8: p. 26-31.*